IAC-15-B4.2.8

LABORATORY PERFORMANCE OF X-RAY DETECTOR ON 2U CUBESAT BEEAGLESAT

Assoc. Prof. Dr. Emrah Kalemci
Sabancı University, Turkey, ekalemci@sabanciuniv.edu

Prof. Dr. Alim Rüstem Aslan
Istanbul Technical University, Turkey, aslanr@itu.edu.tr
Mr. Mustafa Erdem Bas
Istanbul Technical University, Turkey, erdem.bas@itu.edu.tr
Mr. Mehmet Deniz Aksulu
Istanbul Technical University, Turkey, aksulum@itu.edu.tr
Mr. Isa Eray Akyol
Istanbul Technical University, Turkey, akyoli@itu.edu.tr
Mr. Mehmet Sevket Uludag
Istanbul Technical University, Turkey, uludagm@itu.edu.tr

A CdZnTe based semiconductor X-ray detector (XRD) and its associated readout electronics has been developed by the Space Systems Design and Testing Laboratory of Istanbul Technical University and the High Energy Astrophysics Detector Laboratory of Sabanci University along with an SME partner. The XRD will be the secondary science mission on board BeEagleSat, which is developed as one of the double CubeSats for the QB50 project. QB50 is a European Framework 7 project carried out by a number of international organizations led by the von Karman Institute of Belgium.

The heart of the XRD is a 2.5 mm thick, 15 mm x 15 mm CdZnTe crystal with orthogonal electrode strips on top and bottom for position resolution on the crystal. There are 3 sets of steering electrodes in between anodes. A commercial off the shelf (COTS) high voltage source provides necessary potential difference to transport electrons and holes towards electrodes. The signals from each strip are read by a COTS ASIC, RENA-3b, controlled my MSP 430. The XRD board (single ~10 cm x 10 cm board) also carries the necessary power regulators and 7 COTS batteries. In a previous paper presented at the IAC 2014, we discussed the main design of the XRD and provided results from some of the early vibration tests of the mechanical design. At the time, the CdZnTe crystal has not been attached, and the readout electronics and software were still in development phase. In this paper, we present the laboratory performance of the electronic readout system and discuss the current phase of the XRD development.

I. INTRODUCTION

Nano and micro size satellites are becoming an important part of overall satellite development efforts (around 50% [1]) thanks to establishment of the CubeSat standard [2] allowing cheaper yet sophisticated systems being built mostly by universities all around the world. The advantages of CubeSats also attract space agencies, these agencies not only support universities in their efforts, but also design and develop their own systems. Increased use of CubeSat capabilities is also one of the aims of European Framework projects.

QB50 is such a European Framework Program 7 (FP7) project led by the von Karman Institute of Belgium (VKI). QB50's scientific objective is to study the temporal and spatial variations of a number of key constituents and parameters in the lower thermosphere.

A network of about 40 double CubeSats and about 10 triple CubeSats are being built by a number of institutions all around the world. When launched, they will be separated by few hundred kilometers and will make measurements with a pre-determined set of sensors (www.qb50.eu).

BeEagleSat is one of the 40 double (2U) CubeSats which is designed and realized by Istanbul Technical University (ITU), Turkish Air Force Academy (TurAFA) and HAVELSAN, a defense contractor. MicroSMEs Ertek Space and Gumush Space, spin off companies of ITU Space Engineering, also contribute to the overall project.

CAD drawing of the BeEagleSat showing its subsystems is given in Figure 1. QB50 management provides the main payload, the "Multi Needle Langmuir
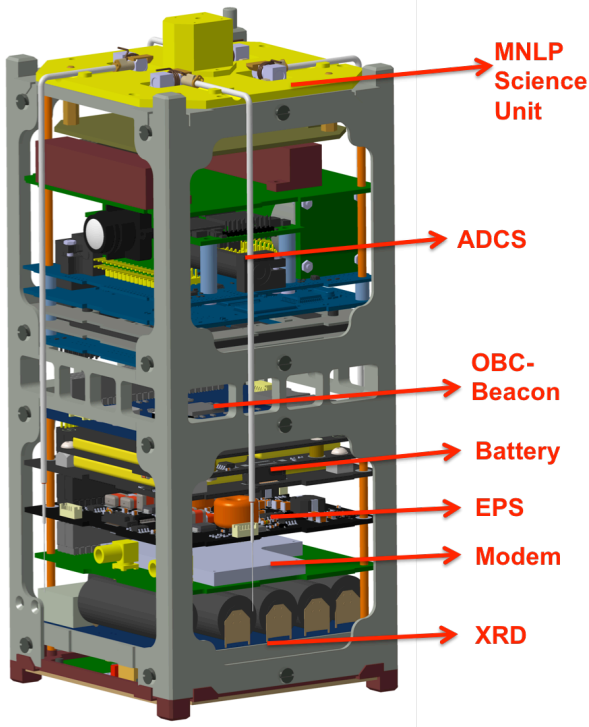
Fig. 1: BeEagleSat drawing and major subsystems.

Probe and Thermistors" (Sensor Set 3). Sabancı University High Energy Astrophysics Detector Laboratory (HEALAB), together with students from ITU Space Systems Design and Testing Laboratory (USTTL) has built a novel X-Ray detector (XRD) as a secondary payload. The BeEagleSat utilizes the QB50 ADCS system [3], a COTS electrical power system (EPS, 3rd Generation from Clyde Space) and modem (Astrodev He-100). The rest of the systems are developed in house based on the mass, volume, link and pointing requirements of the QB50.

In the Proceedings of the 14th International Astronautical Congress (2014, Toronto, Canada), we have described the initial design and components of the XRD, the secondary science payload [4]. In this paper, we will first describe the system again, focusing on the changes occurred since the publication of [4]. The XRD consists of an orthogonal strip CdZnTe crystal (II.I), an application specific integrated circuit (RENA-3b ASIC) for readout, control electronics (II.II), electrical power system (including its own non-rechargeable batteries, high voltage (HV) supply and associated coupling circuits (II.III). We will describe the mechanical design in II.IV, and software, data format and communication with the OBC in II.V. Section III will be devoted to laboratory performance of the electronic readout system where we also discuss issues related to noise.

II. X-RAY DETECTOR ON BEEAGLESAT

CdZnTe semiconductor detectors have been tested and utilized in space. These hard X-ray (20 - 200 keV) detectors for astrophysics can utilize a coded mask and a large number of semiconductor crystals in the focal plane (such as the 32,768 CdZnTe crystals on Swift-BAT [5]), or specially coated X-ray telescope arrays and a fine-pitch large area pixelated detectors (such as the 21 x 21 x 2 mm pixelated CdZnTe crystals on NuSTAR [6]). Pixellated configurations require a large number of readout channels.

CdZnTe and CdTe detectors have been utilized not only in large area detectors on mid- and large-size satellites (such as the Swift, NuStar and the INTEGRAL [7]), but also tried in smaller CubeSats systems. The two examples that we know of are the AAUSat-2 [8], and The Cosmic X-Ray Background Nanosat, CXBN [9]. While AAUSat-2 has single-channel readout, the CXBN utilizes 16 x 32 grid with 600 x 600 μm pixels and two on board calibration sources with a custom made read-out integrated circuit directly bonded to the detector pixels [10]. The thickness of the crystal is 5 mm because it is intended to measure mostly gamma-rays.

BeEagleSat utilizes orthogonal strips for position resolution on a relatively thick CdZnTe crystal (2.5 mm). 15 anode and 15 orthogonal cathodes segment the crystal into 225 pixels with only 30 readout channels, saving precious power and space in a CubeSat. The disadvantage of strip detectors compared to pixellated detectors is the poor energy resolution and higher minimum detectable energy. The XRD on BeEagleSat will demonstrate that orthogonal strip detectors can be utilized in space for astrophysical purposes, and will perform this demonstration with all COTS components (except the crystal). If successful, the XRD will measure the high energy X-ray background at a range of altitudes at low Earth orbit of the BeEagleSat.

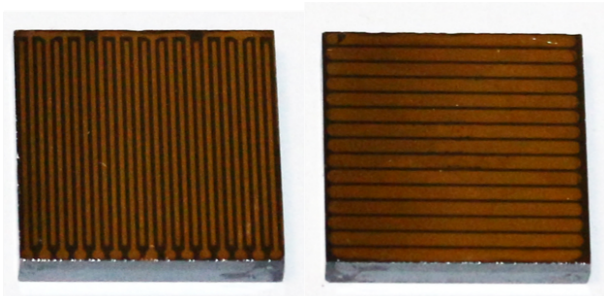In the following subsections, we give a detailed description of the XRD and its tests.

Fig. 2: Left: Anode and steering electrode pattern (1.2 mm pitch) on a 15 x 15 x 2.5 mm IMEM crystal. Right: Cathode strips.

II.I CdZnTe crystal with orthogonal strip configuration

We use a CdZnTe crystal prepared at Due2Lab[*] in Parma, Italy. This is a single crystal with good spectroscopic properties grown at IMEM by the boron oxide vertical Bridgman technique. Details of the crystal growth and spectral properties can be found in Zappettini et al. 2008 [11].

The crystal has been cut to dimensions of 15 x 15 mm with a thickness of 2.5 mm. It is polished and chemically treated for surface passivation. Gold strips are deposited on both sides of the detector orthogonally with a pitch of 1 mm (see Figure 2 for pictures of the anode and cathode sides of the crystal before it was attached to the board). The side that faces the PCB has 15 anode strips that are 0.25 mm wide and kept at ground potential. There are 3 sets of steering electrodes (also 0.25 mm wide) between the anode strips. They are kept at a lower potential (10% of the cathodes) to steer electrons towards the anodes, and their presence also enhances energy resolution due to small pixel effect [12, 13]. The electrode and steering electrode widths are optimized using extensive charge transport and collection simulations and experiments at HEALAB.

Figure 3 shows the current version of the XRD with the crystal attached to the board. The anodes are glued to the pads on the board with conductive epoxy EPO-TEK H20E. The crystal is then glued to the board using a space qualified insulating epoxy (3M 2216 B/A) for structural integrity and damping vibrations (see results of early vibration tests in [4]). On the opposite side, there are 15 orthogonal cathode strips that are 0.8 mm wide and are kept at -250V. The cathode signals and high voltage are transmitted using gold wires from the crystal to the board. Both the anodes and the cathodes are AC coupled to the RENA ASIC through coupling capacitors.
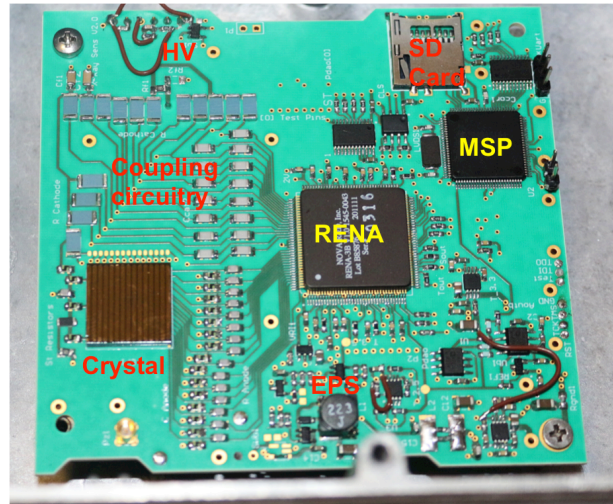
[*] www.due2lab.com/detectors.html

Fig. 3: Picture of the flight model. Some important components are shown on the picture. Crystal is attached, but the cathode wires have not been soldered yet.

II.II Readout circuitry

A single commercially available RENA-3b ASIC performs the initial readout of all anode and cathode strips (see Figure 3). RENA is a low-noise, 36-channel, self-trigger, self-resetting charge sensitive amplifier/shaper integrated circuit [14]. While it has never been tested in space, its low power consumption of <6 mW per channel and use of submicron CMOS process for fabrication are well suited for small satellite applications. Its TVAC tests are soon to be conducted at ITU USTTL.

A MSP 430 microcontroller configures, controls and reads the analog outputs of the RENA chip. Since each channel can be individually configured for polarity, threshold, gain and shaping time, a single chip can read both anode and cathode strips. Once configured, signals exceeding the thresholds trigger the system. RENA sends the list of triggered channels to MSP 430, and then the MSP sequentially reads the analog outputs of triggered channels waiting at the peak & hold circuitry. The analog outputs are read directly at the ADC of the MSP with a resolution of 12 bits.
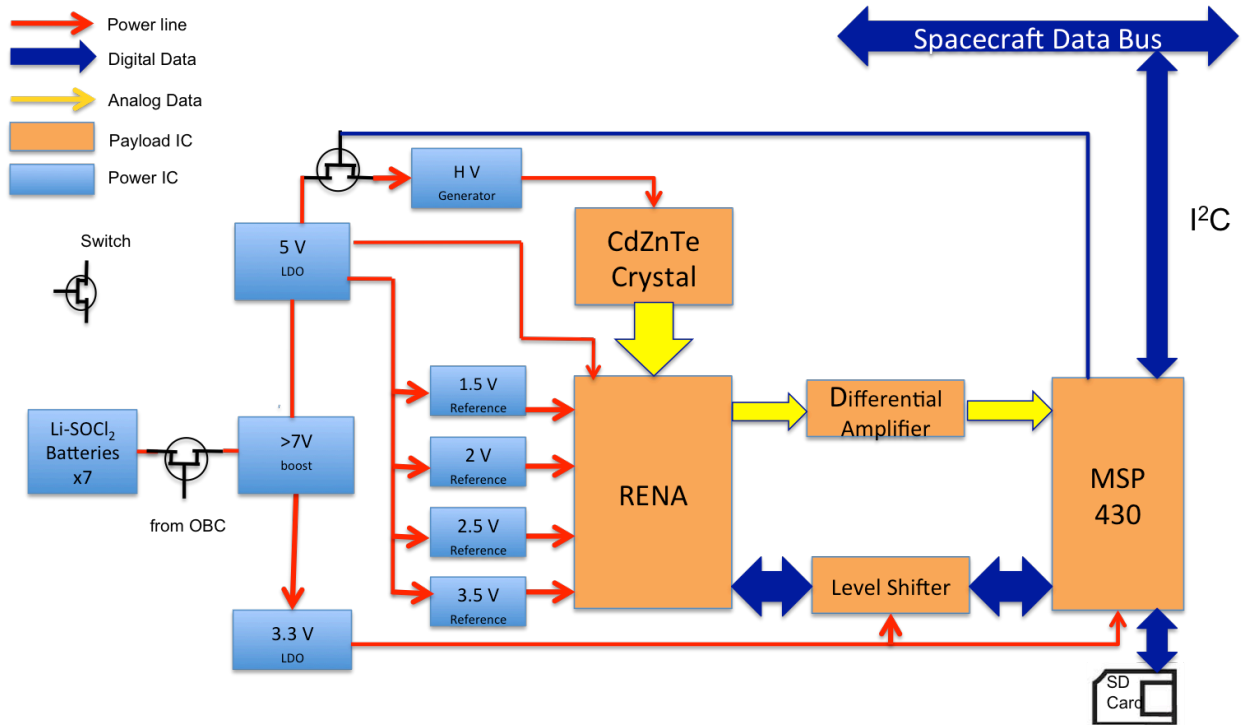
Fig. 4: Electrical block diagram and data flow diagram of the XRD. The entire system can be turned on by the OBC. MSP can only turn on/off the HV supply.

II.III Electrical power system

7 non-rechargeable Li-SOCl2 batteries from SAFT [15] power the independent EPS of the XRD. The system will be turned on intermittently at different altitudes for maximum scientific gain while saving power. The electrical block diagram can be seen in Figure 4. There are several changes in the power management compared to the last design [4] to obtain better noise performance. On board computer (OBC) of the BeEagleSat can turn on and off the entire system at the boost. RENA requires 4 reference voltages to operate, 1.5V, 2V, 2.5V, 3.5V and also 5V for power. MSP can control the operation of the HV generator, it is turned on only during data acquisition.

We are using UltraVolt US series HV supply to provide -250 V to cathodes. This HV supply provide low ripple and performed well in TVAC tests [4].

II.IV Mechanical design

The final XRD (Figure 3) board has been designed and produced as 6 layer PCB board using ROGERS material. Batteries will be attached to one side of the board. (Earlier tests with a mechanical replica showed that this configuration of batteries is stable under vibration tests [4]).

To protect the optically sensitive CdZnTe crystal from Sunlight and any other stray light, the side of the PCB that the crystal is attached to is covered with an aluminium enclosure thick enough to prevent optical light but allowing most of radiation above 20 keV. The CAD drawing in Figure 5 shows how the cover and batteries would looks like.

II.V Control and software

Based on extensive testing and communication with the OBC Software Team (head by HAVELSAN), control and readout software has been simplified compared to version discussed in [4]. The communication with the OBC will take place via I^{2}C port at 400 kHz. The system will be turned on and off by the OBC via a switch at the input boost. The simplified flow diagram is given in Figure 6.

XRD can be driven into 3 operation modes by the commands from the OBC: "IDLE/SAFE MODE", "DIAGNOSTIC MODE", and "DATA ACQUISITION MODE". Before OBC releases the command to drive XRD to one of these modes, it checks if the MSP is functional through the I^{2}C port. This check is performed up to 5 times.
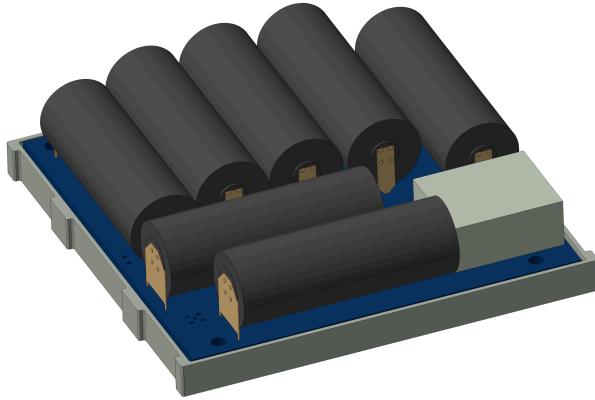
Fig. 5: CAD Drawing of the XRD with the batteries, HV supply and the aluminium cover.
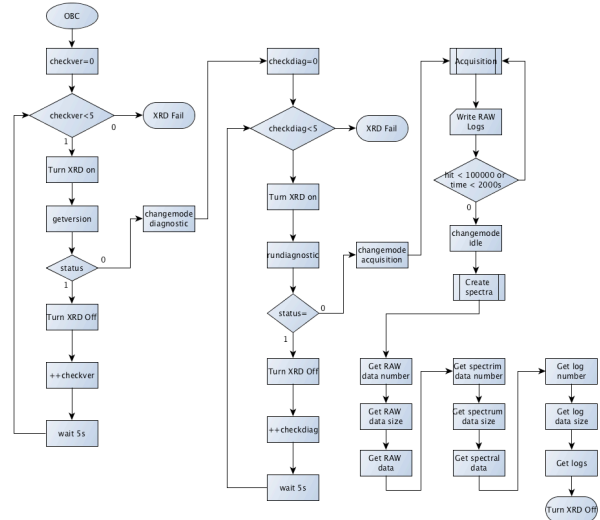

Fig. 6: Basic, simplified flow diagram of the operation.

In the IDLE/SAFE MODE, the HV is turned off and RENA is idle, all channels are turned off to save power.

The current version of the DIAGNOSTIC mode only checks whether RENA receives configuration correctly by reading the threshold voltage of RENA channel 0, which can be set through the configuration. If diagnostic mode fails, the XRD is turned off, and this test repeats up to 5 times before shutting XRD off completely.

The main mode of operation is the "DATA ACQUISITION MODE". In the current, simplified version of this mode, a pre-determined (through ground readout tests) configuration is loaded into RENA and trigger is allowed. RENA takes a pre-determined amount of data (currently 100,000 hits), or stops at timeout (currently 2000 s). The raw data is written to the SD card for every 10 hits due to limitations of the MSP RAM.

The raw data consists of anode and cathode strips that are hit for each trigger, and the signal on each strip.

After data acquisition is finished, raw data is converted into spectrum (see [4] for details of how ground calibration will be done). For diagnostic purposes on ground, we plan to keep some of the raw data. But due to limited telemetry allocation to the XRD, most of the raw data will be categorized and histogrammed to create spectra. The categorization is again based on maximizing science output. Real X-ray events should normally trigger 1 (single) or 2 (double) anodes and 1-3 cathode strips. For deep events, it is possible that only anodes are triggered, but not the cathodes (anode-only). All events that are not singles, doubles or anode-only will be discarded, only their rate

will be saved for diagnostic purposes. Therefore, each time XRD goes into DATA ACQUISITION mode, 5 files are created in the SD card: Raw Data, singles spectrum, doubles spectrum, anode-only spectrum and logs reporting the results of diagnostics, rates of different types of events. Once all the files are created, XRD waits for OBC commands to release data.

The OBC checks and records lengths of spectra and log files, and then transfers parts of different types of data between the given start and end bytes. Once transfer finishes, OBC turns the XRD off until the next acquisition.

III. LABORATORY TESTS

The laboratory tests of the flight module will be presented in 5 subsections: Configuration and data acquisition, EPS, HV and power consumption, noise, and software.

III.I Configuration and data acquisition

RENA is configured by sending a 41 bit configuration sequence for each channel. This configuration sets whether the individual channel is on/off, whether the channel triggers on electrons/holes, sets gain (5 possible gains), input capacitance (low/high), threshold DAC value, and shaping time (5 possible shaping times). Currently, this configuration is prepared and sent by a PC through an interface. Under operating conditions, the pre-determined configuration(s) will be part of the control software, and the MSP will send the particular hardwired configuration.

We tested whether we can correctly configure the ASIC using the MSP. RENA has analog test outputs for 2 channels to check if the pre-amplification and the peak-hold circuits work as expected. Using these test pins, we have determined that RENA receives the configuration correctly. Some of the tests we applied were to change threshold (which we can measure directly, and use it as the main diagnostic), to change gain, turn on/off the channel and change input capacitance. RENA responded to all of these changes as expected, therefore we are confident that we can configure RENA correctly.

The initial configuration had a gain of 5, a shaping time of 1.9 µs and a low input capacitance. This configuration works well for calibration and measurements at HEALAB with the RENA Test Board acquired from NOVA R&D. Unfortunately, due to high noise levels (see section III.III), we had to set trigger threshold quite high, even when a single channel is turned on. Nevertheless, with high enough pulser signals and high enough threshold, we were able to confirm that RENA triggers on pulser, and finalized our data acquisition software which receives list of triggered channels and reads out the analog outputs. We checked the software by turning on/off channels, changing pulser levels, and comparing analog outputs at RENA with the ADC values recorded at the MSP. We have confirmed that RENA operation is as expected during data acquisition, and we can obtain correct list of triggered channels (which is further confirmation that the configuration is sent correctly) and correct ADC values compared to the RENA analog output.

When multiple channels are turned on, cross-talk between channels kicks in, and when all channels are turned on, noise dominates over even the highest threshold level in RENA. See Section III.III about the changes we applied in configuration to mitigate this problem.

III.II EPS, HV and power consumption

We made some changes in the electrical power system hoping to reduce the noise that has been affecting our performance since the earlier tests. We have decided to use a single boost at the entrance to increase battery voltage to ~7V, and then create all other necessary voltages via low-noise LDO regulators. The advantage of this design is to have a single, high noise switching supply at the XRD input, but very low noise filtered potentials at RENA (see Figure 4). As usual, we ordered a few different regulators for each voltage, and individually tested them and chose the ones showing the best performance in terms of noise. They provide nominal voltage levels as required by RENA and other circuits.

The HV source is also soldered and tested. We confirmed that it can be turned on/off by the MSP and provides -250 V to anodes and -25V to steering electrodes as intended.

We checked total power consumption levels to estimate the lifetime of the XRD with the batteries attached. At nominal battery voltage of 3.6V, with no HV and no configuration sent to RENA, the system draws 190-200 mA initially, and settles down to 170-180 mA in a few minutes. Turning on HV has no effect on the current drawn. Note that the crystal has not been attached when these tests have been conducted. If the surface passivation of the crystal prevents excessive surface currents, HV should not draw any current that is high enough to affect system performance.

By sending appropriate configurations we turned on channels slowly and measured the change in current. After the configuration is sent, without any channels turned on, system draws 200-210 mA, and when all channels are turned on, it draws ~290 mA. We determined that each channel draws ~2.5 mA. However, during the time that the data is written to the SD card, system draws substantially more current. It is difficult to determine exactly how much current the SD card draws as the writing process takes only a few ms and our measuring device cannot update that quickly. To get a better sense of SD card current, we altered the software to continuously write to SD card so that what we measure as an average is close to the instantaneous current. We measured ~100 mA difference, and assumed that this is the instantaneous current that the SD card writing process draws.

We measured the time it takes from the trigger to writing the raw data to buffer as 712 µs+20 µs/channel. Assuming 5 channels triggering on average, each hit takes ~0.8 ms. The RAM of the MSP must be written to the SD card for every 10 hits and this process takes 26 ms. Therefore, how much current the system draws and the lifetime of the XRD depends critically on the count rate. For low count rates (1-2 cts/s) duty cycle of writing to SD card will be small and on average the system will draw 300 mA. If the count rate is 50 cts/s, the duty cycle of writing to SD card becomes ~10%. Higher count rates will result in higher average currents, and higher dead time at the same time. Assuming we hit timeout at 2000 s for each XRD run, a count rate of 50 cts/s, 50% for the average efficiency of the batteries (~1.7 Ah per battery) we estimate that the system can be turned on intermittently 70 times. Note that we also assumed that the time it takes to convert raw data to

spectrum and to transfer data to the OBC are negligible compared to acquisition time. Lowering acquisition times will increase the number of times we can operate the XRD, however, this may result in too few counts to produce a statistically significant spectrum. We will be able to telemetry data every other day.

III.III Noise

Noise at the RENA outputs has been the primary obstacle we have been dealing with since the beginning of our tests. The test board discussed in [4] has been modified for our efforts to reduce noise. We changed the PCB stacking, PCB material and made sure that each RENA input has 2 bypass capacitors. We also fixed some design issues from the previous version and re-produced the PCB.

Changing the EPS design did not help. The power supply at the boost produced noise spikes during switching, and we observed switching frequency noise leaking to ground and outputs of all regulators. To test whether the input boost is the ultimate reason for the noise at RENA, we disconnected it and used an external power supply instead. While it removed the switching spikes, the noise at RENA amplifiers persisted. Up to now, all of our efforts to determine the source of this noise and our suggested fixes have failed. While there are other possibilities that we would like to try to reduce noise, the expected launch date of BeEagleSat places a tight constrain for substantial changes in the design and production.

For this reason we decided to compromise from the science case of measuring sky background in 20-200 keV range, and concentrate on running the system, obtaining data and testing software. To be able to do that we changed the default configuration such that the gain is 1.1 and the input capacitance is large. These choices reduced the baseline level of noise at the shaping amplifier, allowing us to set a meaningful threshold for trigger. For each channel, we determined the threshold for which the system does not trigger on noise and recorded these thresholds into the default configuration file. This effectively means that the RENA is now sensitive to only very high energy events and energetic cosmic particles. While this is not the initial intent of the project, it will allow us to detect photons and particles at higher energies while learning valuable lessons in producing a payload that functions.

III.IV Software

The description of the software is given in Section II.V. Up to now, the configuration and data acquisition software have been written and tested thoroughly in the lab. The data format is finalized, and commands to write raw data to the SD card have also been tested and verified. Initial tests of the spectrum creation routines have been performed. The data format for the spectra is finalized. The commands for communication with the OBC through the I^2C have been finalized and all of them have been tested.

IV. CONCLUSION and FUTURE WORK

We developed a 2U CubeSat (BeEagleSat) with contributions from ITU, TurAFA, HAVELSAN and SU. The BeEagleSat will be part of the QB50 Network hosting sensor Set 3. More importantly, a local X-Ray detector system will be space qualified. At the time of writing this proceeding, the XRD received its final element, the CdZnTe crystal, and is now ready for full acceptance tests. Control, readout and communication software have already been tested. The EPS and operation of the RENA ASIC are verified. The software and hardware operate with a level of noise that is too high for the original science objectives of the payload. While we still continue to search for the cause of this problem, we changed the configuration to allow larger energy photons and particles to trigger the system.

Before we can deliver the XRD module, a number of tests have to be conducted. A re-characterization of the noise will be done with the aluminium cover and power provided by batteries, with no external connection to the PCs. This will provide the true level of noise and help us finalize the configuration settings. Next step is ground calibration, which will be done with a Cs radioactive source. The calibration parameters will be hard wired to the software that creates spectra and software for creating spectra will be tested. Finally standard TVAC and vibration tests will be performed with the entire subsystem inside the CubeSat.

V. ACKNOWLEDGMENTS

REFERENCES

[1] E. Buchen, and D. DePasquale, "2014 Nano /Microsatellite Market Assessment", SpaceWorks Enterprises, Inc. (SEI) , Atlanta, GA

[2] CubeSat Design Specification, Rev.13, The CubeSat Program, Cal Poly SLO.

[3] W.H. Steyn and M. Kearney., "An Attitude Control for ZA-AeroSat Subject to Significant Aerodynamic Disturbances", 19th World Congress of the International Federation of Automatic Control, 2014, August 24-29, Cape Town, South Africa.

[4] R. Aslan et al. "Development and in orbit testing of an X Ray Detector within a 2U CubeSat", Proceedings of the 65th International Astronautical Congress, 2014, Toronto, Canada.

[5] S. Barthelmy, et al., "The Burst Alert Telescope (BAT) on the SWIFT Midex Mission", Space Sci. Rev., 120, p. 143, 2005.

[6] Harrison, F.A., Craig, W.W., Christensen, F.E., et al. "The Nuclear Spestroscopic Telescope Array (NuSTAR) High-Energy X-Ray", ApJ, 770, 103., 2013

[7] LeBrun, F. et al. "ISGRI: The INTEGRAL Soft Gamma-Ray Imager" A&A, 411, L231

[8] https://directory.eoportal.org/web/eoportal/satellite-missions/a/aausat-2

[9] https://directory.eoportal.org/web/eoportal/satellite-missions/c-missions/cxbn

[10] L. M. Simms et al., "CXBN: a blueprint for an improved measurement of the cosmological x-ray background" Proc. SPIE 8507, p19, 2012.

[11] A. Zappettini et al., "Boron oxide encapsulated vertical Bridgman grown CdZnTe crystals as X-ray detector material", Nuclear Science Symposium Conference Record, 2008. NSS '08. IEEE, p. 118, 2008.

[12] E. Kalemci & J. L. Matteson, "Charge Sharing among the electrodes of a CdZnTe detector", NIM-A, 478/3, p529, 2002.

[13] E. Kalemci et al., "Model calculations of the response of CZT strip detectors", Proc. SPIE 3767, p.360, 1999.

[14] T. O. Tumer, et al., "Performance of RENA-3 IC with Position-Sensitive Solid-State Detectors", Proc. SPIE 7079, p.70791F, 2008.

[15] Saft Battery datasheet - http://www.saftbatteries.com/doc/Documents/primary/Cube655/LS17500_0710.207ec74a-0a3e-4f1a-8f8e-bf5a6150cfd6.pdf